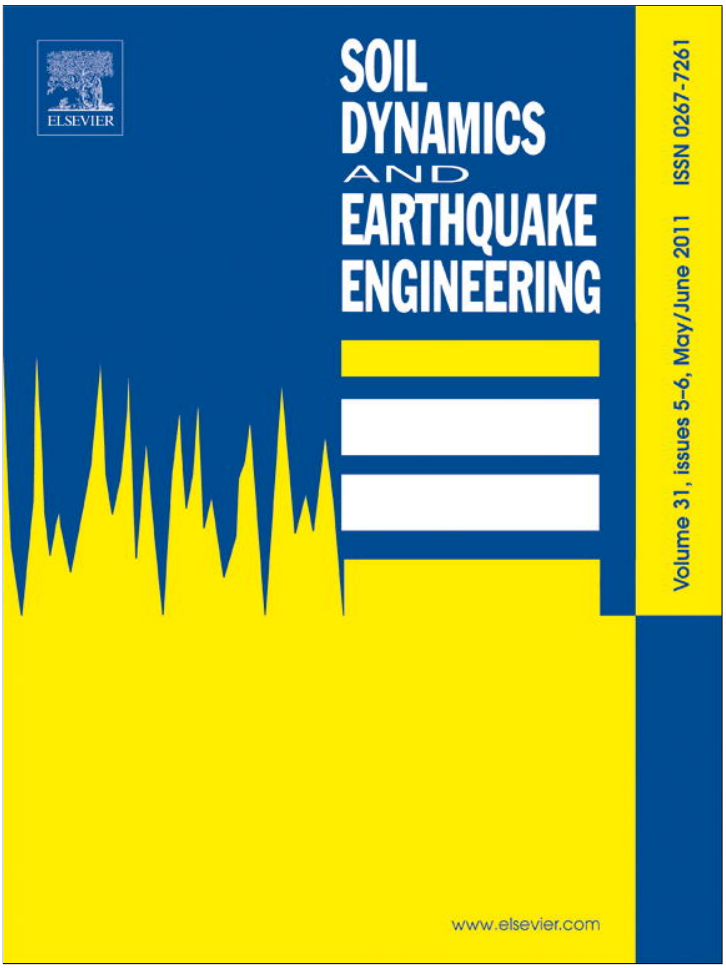

Soil Dynamics and Earthquake Engineering 31 (2011) 805–816

Contents lists available at ScienceDirect

Soil Dynamics and Earthquake Engineering

journal homepage: www.elsevier.com/locate/soildyn

Experimental validation of soil–structure interaction of offshore wind turbines

S. Bhattacharya [a], S. Adhikari [b,*]

[a] Department of Civil Engineering, University of Bristol, Queen's Building, University Walk, Clifton, Bristol BS8 1TR, UK
[b] College of Engineering, Swansea University, Singleton Park, Swansea SA2 8PP, UK

ARTICLE INFO

Article history:
Received 2 August 2010
Received in revised form
17 November 2010
Accepted 9 January 2011
Available online 12 February 2011

ABSTRACT

Estimating the natural frequencies of a wind turbine system consisting rotor, nacelle, tower, foundation and surrounding soil is one of the important design considerations. This paper experimentally investigates the behaviour of a model wind turbine supported on a particular type of foundation called a monopile. Monopile is a single large diameter (2.5–4 m) long slender column inserted deep into the ground. This can be thought of as an extension of the wind turbine tower. In particular, the role of soil/foundation in the dynamics of wind turbines has been investigated. Analytical methods are developed incorporating the rotational and translation flexibility of the foundation. Novel experimental techniques have been developed to obtain the parameters necessary for the analytical model. The analytical model is validated using a finite element approach and experimental measurements. In total, results from 17 test cases is reported in the paper. Experimental results show that the natural frequencies and the damping factors of the wind turbine tower change significantly with the type of soil/foundation. Analytical results for the natural frequencies agree reasonably well to the experimental results and finite element results.

1. Introduction

Offshore wind farms are considered as a viable solution to the energy problem due to many reasons: (a) they are generally located more than 10 km from shore and thus noise, size and vibration effects on humans are alleviated by their distance from land; (b) the average wind speed over water is generally higher, making it more reliable and efficient than a similar onshore wind farm. The foundations for offshore wind turbines are particularly challenging due to the dynamic nature of the offshore loading and the difficulty in the working conditions and as a result, the cost of foundations is quite substantial. Fig. 1 shows the contribution of the cost of foundations to the capital costs for North Hoyle offshore wind farm [1]. The 34% cost of foundations, which includes the installation cost, is rather high if the total amount of materials and work input is taken into consideration. A greater understanding of the behaviour of wind turbine foundations will inevitably lead to the cheaper construction of foundations which, in turn, will make offshore wind farms a more viable part of the solution to the global energy problem. This aim of this paper is to propose a simple approach to take into account the dynamic soil–structure interaction.

Typical foundations either proposed or used in practice to support offshore wind turbines are shown in Fig. 2. Type A refers to monopile type of foundation and while Type B is suction caisson type. Type C is multipod type where three or four suction caisson foundations are used. Type D is a large circular or polygon shaped concrete raft embedded deep into the ground. Fig. 2 also shows a mathematical model which can describe these structures where the foundation is 'replaced' by two types of linear springs as suggested by DnV code [2] of practice:

- k_l (translational spring constant);
- k_r (rotational spring constant).

The linear nature of the springs can be justified by the fact that we are considering essentially small deflection or rotation of the foundation. This research is based on monopile type of foundation. Monopile is increasingly becoming the choice because of its simplicity: see for example the Lely Wind turbine (the Netherlands), Blyth (England, UK), Scroby sand (Norfolk coast, UK) and North Hoyle (Wales, UK).

Designers need to predict the natural frequency of the wind turbine system based on the turbine characteristics, foundation and the soil profile. Tempel and Molenaar [3] studied the problem by idealising the wind turbine as a flagpole of length L, mass per

* Corresponding author. Tel.: +44 1792 602088; fax: +44 1792 295676.
E-mail addresses: S.Bhattacharya@bristol.ac.uk (S. Bhattacharya), S.Adhikari@swansea.ac.uk (S. Adhikari).

0267-7261/$ - see front matter © 2011 Elsevier Ltd. All rights reserved.
doi:10.1016/j.soildyn.2011.01.004

unit length m having an average bending stiffness EI with a top mass M. Although they have proposed a simple equation for the first natural frequency, it does not incorporate the flexibility of the foundation. For a tapering tower (which is usually the case for offshore wind turbines), Tempel and Molenaar [3] recommend the use of the average diameter. Here we outline an analytical formulation to study the dynamics of the problem by incorporating the foundation flexibility through the use of two springs (k_r and k_l). This paper aims to experimentally validate the formulation through well calibrated controlled experiments. Though sophisticated finite element analysis considering superstructure–pile–soil interaction or beam-on-non-linear-winkler foundation model or commercial software such as GH-BLADED may be used to predict the natural frequency of the system, it is considered useful to develop a chart/graph based method for validation purposes. This can be helpful for quick estimation of the natural frequency which is often required in the preliminary design stage. The proposed analytical formulation is also validated against high-fidelity finite element simulation results. In summary, the main objectives of the paper are:

- To develop laboratory based testing methods for the vibration analysis of scaled wind turbine models in different types of soils.
- To develop novel experimental techniques for the determination of soil–structure interaction parameters.
- To validate Euler–Bernoulli beam theory based simplified analytical approach against the experimental measurements.
- To compare the results obtained from the analytical approach, finite element method and experimental measurements.

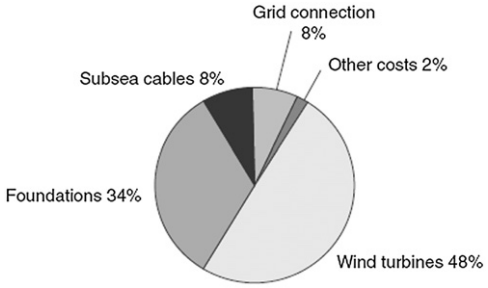

Fig. 1. Cost break down North Hoyle Wind Turbine in North Hoyle. This shows that foundations may cost up to 34% of the total cost of the project. Source Ref. [1].

The outline of the paper is as follows. In Section 2, the free vibration analysis of wind turbines is discussed. The equation of motion and boundary conditions are discussed in Section 2.2. The equation governing the natural frequencies is derived in Section 2.3. The experimental technique developed in this work is described in Section 3. In Section 3.1 the description of the model wind turbine is given. The set-up and procedure for testing is detailed in Section 3.2. Experimental results are discussed in Section 4. Based on the analytical, numerical and experimental studies, a set of conclusions are drawn in Section 5.

2. Brief overview of vibration of wind turbines towers on flexible foundations

2.1. Soil–structure interaction for wind turbines

Dynamic soil–structure interaction for offshore wind turbines is complex due to various interactions between the structure, foundation, soil and the fluid. When the blades start to rotate, dynamic loads are generated in the foundation due to cyclic loading arising due to many effects, for example:

- Any out-of-line imbalances in the nacelle-rotor system at the hub or the flexibility of the long blades can cause an excitation in the tower which in turn applies a cyclic loading on the foundation. Though this is a source of excitation arising from the rotor (denoted by 1P) but this may not be the prominent one for design purpose.
- Another source of excitation is the blade passing frequency due to the tower shadow each time the blade passes the tower. This causes excitation, the frequency of which is given by the multiplication of the number of blades and the rotor frequency.

These dynamic loads cause the pile to oscillate against the soil. As a result stress waves originate at the pile–soil interface and propagate outwards in the form of body waves and surface waves radially propagating towards infinity. The waves would carry away some of the energy in the form of radiation damping. In any cycle of loading in the foundation, the stresses in the soil surrounding the pile would be asymmetric and non-uniform: the soil in the direction of loading will experience more stress. This non-uniform stress distribution will lead to a radial variation in the shear strain and will depend on the direction and magnitude of loading. Under repeated cyclic loading, the behaviour of soils may vary depending on the soil type (sand or clay or mixed soils), moisture content (saturated or dry), frequency of loading (drained

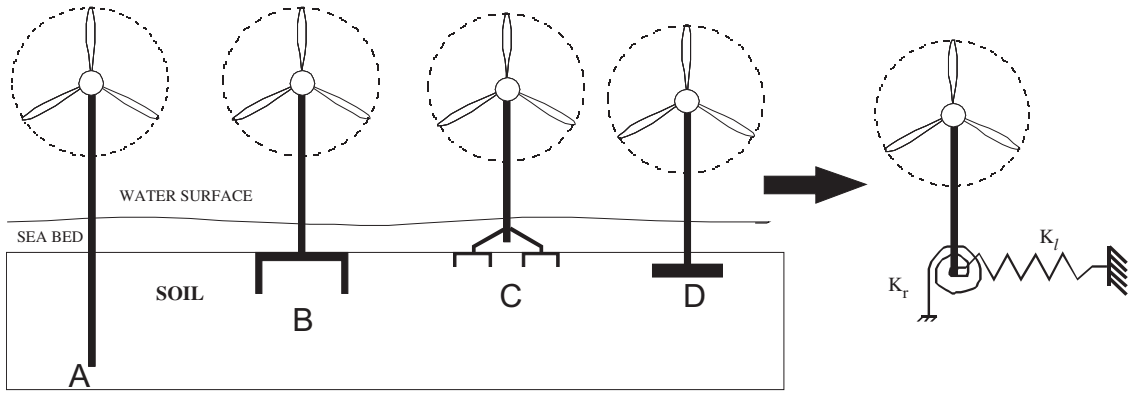

Fig. 2. Different types of foundations to support offshore wind turbines and the proposed mathematical model for analysis. (A) Monopile, (B) suction caisson, (C) multipod and (D) large circular or polygon shaped concrete raft embedded deep into the ground. The translational spring constant k_l and the rotational spring constant k_r are used to simplify the soil–structure interaction. Experimental methods to obtain these two constants are developed in Section 3.

or undrained). For example repeated cyclic undrained loading in loose to medium dense saturated sandy soil may lead to liquefaction as it happens in earthquakes. This will lead to lower pile stiffness, see for example Bhattacharya et al. [4]. Under moderate cyclic loading, most clays degrade in stiffness and this primarily depends on PI (Plasticity Index) of the soil and number of cycles of loading [5]. On the other hand, loose to medium dense dry sandy soil will tend to compact leading to higher pile stiffness.

The change in pile stiffness will alter the natural frequency of the wind turbine-foundation system leading to different response of the pile head, i.e. the pile head deflection would be different from the previous cycle which will induce different amounts of strain in the soil next to it. This incremental change in response depends on the forcing frequency and the natural frequency of the system at that point in time. The damping of the system is also expected to change. One of the aims of the experiments reported in this paper is to verify the hypothesis presented here. For theoretical studies, we use a simple Euler–Bernoulli beam model, as described in the next subsection.

2.2. Equation of motion and boundary conditions

In this study, the wind turbine system is idealised by an Euler–Bernoulli beam with axial force as shown in Fig. 3. A detailed analysis of this model can be found in our previous works [6,7]. Here we briefly outline the necessary details for the experimental validation of this approach. The equation of motion of the beam is given by (see, for example, the book by Géradin and Rixen [8] for the derivation of this equation)

$$EI\frac{\partial^4 w(x,t)}{\partial x^4}+P\frac{\partial^2 w(x,t)}{\partial x^2}-mr^2\frac{\partial^2 \ddot{w}(x,t)}{\partial x^2}+m\ddot{w}(x,t)=f(x,t). \quad (1)$$

Here $w(x,t)$ is the transverse deflection of the beam, t is time, $(\dot{\bullet})$ denotes derivative with respect to time and $f(x,t)$ is the applied time depended load on the beam. In this work we consider motion in the transverse direction only. Motion in the axial direction has not been considered. The height of the structure is considered to be L, with the radius of gyration r. The translational spring constant k_l and the rotational spring constant k_r are used to model the soil–structure interaction. It should be noted that modelling the foundation by springs can be done for any type of foundation with varying accuracy. The four boundary conditions associated with Eq. (1) are given in Table 1. The spring constants affect the boundary conditions at $x=0$.

Eq. (1) is a fourth-order partial differential equation [9] and has been used extensively in literature for various problems (see for example, Refs. [10–19]). In the previous work [6,7] the authors developed a method for the calculation of the natural frequencies of system (1) based on the non-dimensionalisation of the equation of motion and the boundary conditions. Here we briefly review the necessary details. We consider free vibration so that the forcing can be assumed to be zero. Assuming harmonic solution we have

$$w(x,t)=W(\xi)\exp\{i\omega t\}, \quad \xi=x/L. \quad (2)$$

Substituting this in the equation of motion and the boundary conditions one has

$$\frac{\partial^4 W(\xi)}{\partial \xi^4}+\tilde{v}\frac{\partial^2 W(\xi)}{\partial \xi^2}-\Omega^2 W(\xi)=0,$$

$$W''(0)-\eta_r W'(0)=0,$$

$$W'''(0)+\tilde{v}W'(0)+\eta_l W(0)=0,$$

$$W''(1)-\beta\Omega^2 W'(1)=0,$$

$$W'''(1)+\tilde{v}W'(1)+\alpha\Omega^2 W(1)=0. \quad (3)$$

Here the non-dimensional parameters can be identified as

$$\tilde{v}=v+\mu^2\Omega^2,$$

$$v=\frac{PL^2}{EI} \quad \text{(nondimensional axial force)},$$

$$\eta_r=\frac{k_r L}{EI} \quad \text{(nondimensional rotational foundation stiffness)},$$

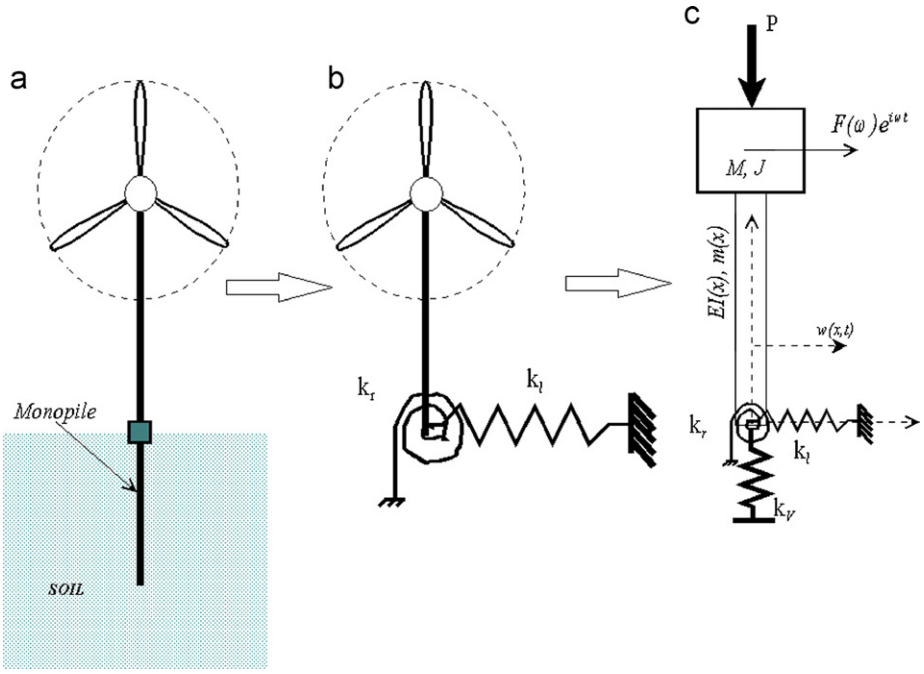

Fig. 3. Mathematical idealisation of a wind turbine tower imbedded in soil by Euler–Bernoulli beam with axial force and end springs k_l and k_r. The height of the tower is L, mass per length m, average bending stiffness EI. The turbine system is idealised by a top mass M with rotary inertia J. The vertical (axial) force on the tower $P=Mg$, where g is the acceleration due to the gravity.

Table 1
Boundary conditions associated with the Euler–Bernoulli beam model.

Boundary conditions	Equations
Bending moment at $x=0$	$EI\frac{\partial^2 w(x,t)}{\partial x^2}-k_r\frac{\partial w(x,t)}{\partial x}=0\Big\|_{x=0}$ or $EIw''(0,t)-k_rw'(0,t)=0$
Shear force at $x=0$	$EI\frac{\partial^3 w(x,t)}{\partial x^3}+P\frac{\partial w(x,t)}{\partial x}+k_lw(x,t)-mr^2\frac{\partial \ddot{w}(x,t)}{\partial x}=0\Big\|_{x=0}$ or $EIw'''(0,t)+Pw'(0,t)+k_lw(0,t)-mr^2\frac{\partial \ddot{w}(x,t)}{\partial x}=0$
Bending moment at $x=L$	$EI\frac{\partial^2 w(x,t)}{\partial x^2}+J\frac{\partial \ddot{w}(x,t)}{\partial x}=0\Big\|_{x=L}$ or $EIw''(L,t)+J\frac{\partial \ddot{w}(x,t)}{\partial x}=0$
Shear force at $x=L$	$EI\frac{\partial^3 w(x,t)}{\partial x^3}+P\frac{\partial w(x,t)}{\partial x}-M\ddot{w}(x,t)-mr^2\frac{\partial \ddot{w}(x,t)}{\partial x}=0\Big\|_{x=L}$ or $EIw'''(L,t)+Pw'(L,t)-M\ddot{w}(L,t)-mr^2\frac{\partial \ddot{w}(x,t)}{\partial x}=0$

$$\eta_l=\frac{k_lL^3}{EI}\quad\text{(nondimensional lateral foundation stiffness)},$$

$$\Omega^2=\omega^2\frac{mL^4}{EI}\quad\text{(nondimensional frequency parameter)},$$

$$\alpha=\frac{M}{mL}\quad\text{(mass ratio)},$$

$$\beta=\frac{J}{mL^3}\quad\text{(nondimensional rotary inertia)},$$

and

$$\mu=\frac{r}{L}\quad\text{(nondimensional radius of gyration)}. \tag{4}$$

We define the natural frequency scaling parameter

$$c_0=\sqrt{\frac{EI}{mL^4}}. \tag{5}$$

Using this the natural frequencies of the system can be obtained as

$$\omega_j=\Omega_jc_0,\quad j=1,2,3,\ldots. \tag{6}$$

2.3. Equation of the natural frequencies

Assuming a solution of the form

$$W(\xi)=\exp\{\lambda\xi\} \tag{7}$$

and substituting in the equation of motion (3) results

$$\lambda^4+\tilde{v}\lambda^2-\Omega^2=0. \tag{8}$$

This is the equation governing the natural frequencies of the beam. Solving this equation, for λ^2 we have

$$\lambda^2=-\frac{\tilde{v}}{2}\pm\sqrt{\left(\frac{\tilde{v}}{2}\right)^2+\Omega^2}=-\left(\sqrt{\left(\frac{\tilde{v}}{2}\right)^2+\Omega^2}+\frac{\tilde{v}}{2}\right),\quad\left(\sqrt{\left(\frac{\tilde{v}}{2}\right)^2+\Omega^2}-\frac{\tilde{v}}{2}\right). \tag{9}$$

Because $\tilde{v}^2$ and Ω^2 are always positive quantities, both roots are real with one negative and one positive root. Therefore, the four roots can be expressed as

$$\lambda=\pm i\lambda_1,\quad\pm\lambda_2, \tag{10}$$

where

$$\lambda_1=\left(\sqrt{\left(\frac{\tilde{v}}{2}\right)^2+\Omega^2}+\frac{\tilde{v}}{2}\right)^{1/2}\quad\text{and}\quad\lambda_2=\left(\sqrt{\left(\frac{\tilde{v}}{2}\right)^2+\Omega^2}-\frac{\tilde{v}}{2}\right)^{1/2}. \tag{11}$$

In view of the roots in Eq. (10), the solution $W(\xi)$ can be expressed as

$$W(\xi)=a_1\sin\lambda_1\xi+a_2\cos\lambda_1\xi+a_3\sinh\lambda_2\xi+a_4\cosh\lambda_2\xi. \tag{12}$$

Applying the boundary conditions in equations on the expression of $W(\xi)$ in (12), the equation governing the natural frequencies can be obtained (see Ref. [6] for details) as

$$[\mathbf{R}(\Omega)]\mathbf{a}=\mathbf{0}. \tag{13}$$

Here $\mathbf{a}=\{a_1,a_2,a_3,a_4\}^T$ and $\mathbf{R}(\Omega)$ is a 4×4 matrix whose elements are nonlinear functions of $\lambda_1,\lambda_1,\eta_r,\eta_l,\alpha,\beta,\tilde{v}$ and Ω. The non-dimensional natural frequencies can be obtained by solving Eq. (13) numerically for Ω. Denoting the solution of this equation as Ω_j, the actual natural frequencies of the system can be obtained using Eq. (6).

2.4. Numerical results

The variation of the first natural frequency of the wind turbine with respect to the nondimensional rotational foundation stiffness for different values of axial force and four fixed values of the nondimensional lateral stiffness is shown in Fig. 4. A similar result (not shown here) can be obtained for the variation of the first natural frequency with respect to the nondimensional lateral foundation stiffness for different values of axial force and four fixed values of the nondimensional rotational stiffness. The salient features of the analysis carried out here can be summarised as follows:

- The natural frequency of the system increases with the increasing values of the stiffness parameters η_l and η_r. This is due to the fact that the increase in the rotational and lateral stiffness properties stabilises the system. It may be noted that after certain values (typically above 100), a further increase in their values do not change the natural frequency. This is because after these values, the foundation structure interaction can be essentially considered as fixed and further increase in η_l and η_r and has no effect.
- The natural frequency of the system decreases with the increasing value of v, i.e. non-dimensional values of axial force on the tower. This is expected as the increase in the downward axial force essentially drives the system closer to axial instability (buckling).
- Since the results are in terms of the generalised non-dimensional quantities, they are applicable to any turbine structures which can be modelled within the scope of the theory discussed here.

In the next section, an experimental method is proposed to validate the simplified analytical approach discussed in this section.

3. Experimental technique

3.1. Description of the model wind turbine

A 1:100 scale model of a Vestas V90 3 MW wind turbine which has a swept area diameter of 90 m and a nacelle height of 105 m has been developed in BLADE laboratory of the University of Bristol (see Fig. 5 for a photograph and a schematic diagram). The details of

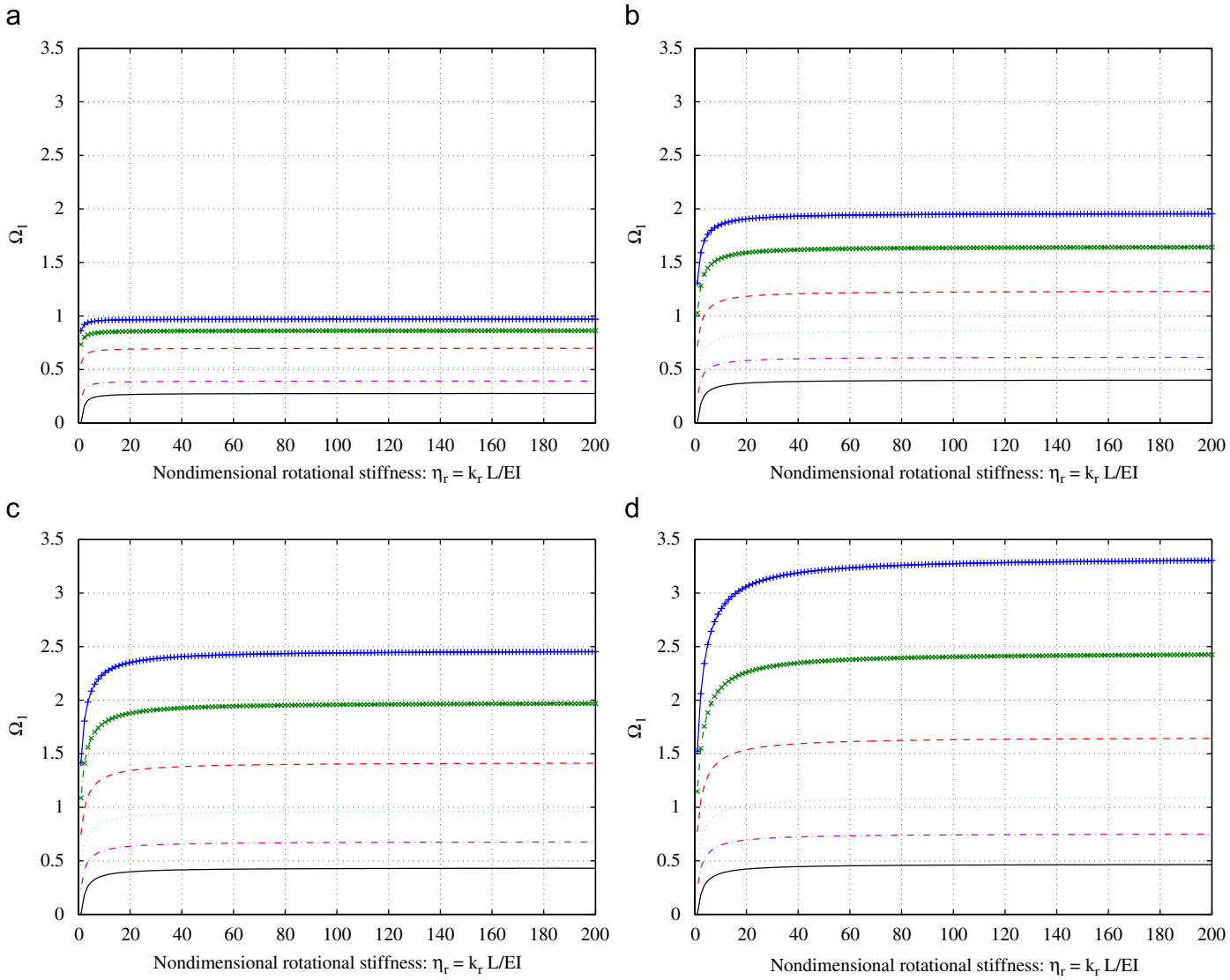

Fig. 4. The variation of the first natural frequency of the wind turbine with respect to the nondimensional rotational foundation stiffness η_r for different values of nondimensional axial load v. Four fixed values of the nondimensional lateral stiffness η_l are considered in the four subplots. '-+-' $v = 0.001$; '-.x-.' $v = 0.03$; '––' $v = 0.1$; ' . . . ' $v = 0.25$; '-.-.' $v = 0.5$; '—' $v = 0.5$. (a) $\eta_l = 1$; (b) $\eta_l = 5$; (c) $\eta_l = 10$; (d) $\eta_l = 100$.

the model wind turbine along with the parameters are given in Table 2. The model wind turbine blades are constructed from a lightweight wood and are attached to a 24v electric motor powered by a DC power supply which is then attached to the tower. The effect of rotor frequency (1P) is simulated through the revolutions of the blades powered by the motor. A displacement controlled actuator has been employed which acts at a point in the tower to simulate the wind loading on the structure: mainly the blade passing frequency (3P). Monopile type of foundation has been used as shown in Fig. 2(a). The various parts of the wind turbine can be disassembled easily which allowed separate test to be carried out on the monopile alone. The lateral foundation stiffness (k_l) and the rotational foundation stiffness (k_r) are evaluated by direct measurements as discussed in the next section.

The derivation of the correct scaling laws constitutes the first step in an experimental study. These are necessary to interpret the model test results and scale up the results for true scale prototypes. Most of the physical process can be expressed in terms of non-dimensional groups and the fundamental aspects of physics need to be preserved in the design of model tests. The physical mechanisms that are considered important in order to develop the non-dimensional groups are based on the following:

- It is well known that the strain field in the soil around a laterally loaded pile controls the degradation of soil stiffness. This can also be linked to the cyclic stress ratio in the soil in the near field shear zone.
- The frequency of the vibration is proportional to the rate of soil loading which will influence the dissipation of pore water pressure for fine grained soils.
- As these are dynamically sensitive structures, the system dynamics, i.e., the relative spacing of the system frequency (soil–structure interaction or SSI frequency) and the loading frequency need to be maintained.
- Bending strain in the monopile foundation needs to be considered for thin walled pile section to account for the non-linearity in the material of the pile.
- Fatigue in the monopile foundation can also be a design issue.

Table 3 shows the dimensional groups that can be used to scale the test results to predict prototype performance. However, this is

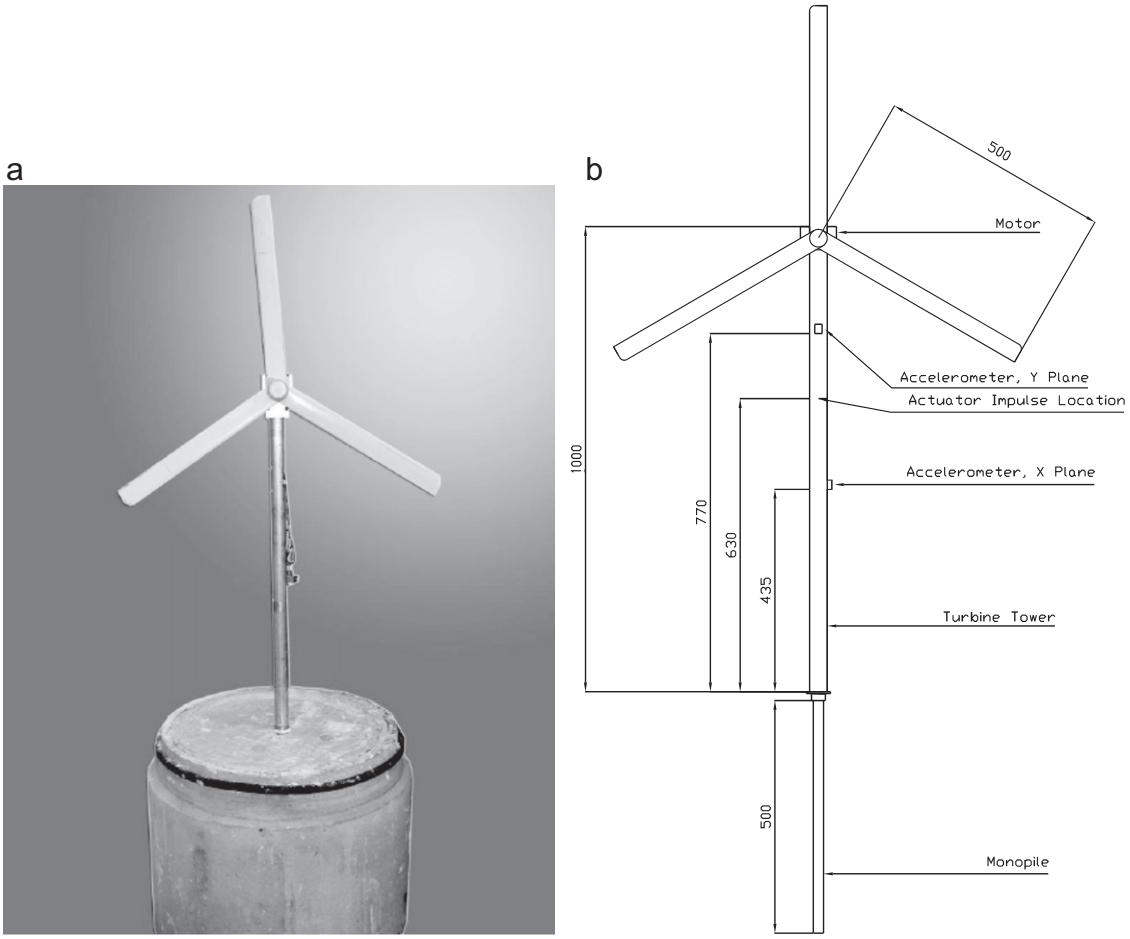

Fig. 5. A photograph and a schematic diagram of the model wind turbine structure used in this study. (a) The model wind turbine on a foundation. (b) Schematic diagram of the turbine showing the locations of the accelerometer and the actuator. The dimensions are in mm.

Table 2
Details of the model wind turbine.

Parameters	Values	Remarks
EI (tower)	2.125×10^9 N mm^2	Bending rigidity of the tower (tower diameter 38 mm)
M (mass of the rotor and blades)	1.348 kg	Motor weighs: 1.008 kg and the blades 0.34 kg
Length of the tower (L)	1.0 m	Aluminium tube of 38 mm dia. and 1.6 mm thickness
m (mass per unit length of the tower)	0.576 kg/m	Uniform tube (non-dimensional axial force)
v	0.006	Here $P = 1.348 \times 9.8$ N $= 13.2$ N
$c_0/2\pi$	11.46 Hz	Here EI is that of the tower
Non-dimensional mass ratio α	2.34	$M = 1.348$ kg and $mL = 0.576$ kg
Frequency of the system fixed at the base of the tower	10.66 Hz	This is calculated based on Eq. (14). The measured value is 10.27 Hz
Pile length	0.5 m	These data are not directly relevant in this research but are provided for the sake of completeness
EI (pile)	3.18×10^8 N mm^2	Bending rigidity of the pile (pile diameter 22 mm)

Table 3
Scaling laws for the model wind turbine. P, total lateral load on the wind turbine; G, shear modulus of the soil at a reference height; D, pile diameter; f, forcing frequency; K_h, horizontal permeability of the soil; f_{sys}, system frequency; y, point of application of the total load; t, thickness of the pile; E, Young's modulus of the pile; σ_y, yield stress of pile material.

Non-dimensional group	Physical meaning
P/GD^2	Similar strain field in the soil around the pile ensuring similar degradation of soil stiffness
Df/k_h	Similar rate of loading. Modelling consolidation/dissipation of pore water pressure
$f : f_{sys}$	Relative spacing of the forcing frequencies and the natural frequencies, i.e. system dynamics
Py/ED^2t	Strain level in the pile. Non-linearity in the pile
$Py/\sigma_y D^2 t$	Stress level in the pile. Fatigue limit state

beyond the scope of the paper as the main aim is to validate the analytical model. We refer the paper by Bhattacharya et al. [20] where certain aspects of the scaling laws are presented.

The wind turbine was founded on various types of soils: dry sand, saturated sand, and soft clay. The sand used in the experiments is Leighton Buzzard Fraction B sand conforming to BS 1881-131:1998. The properties are given in Table 4. The properties of the soils used in the test are given in Table 5. Two accelerometers were fitted to the turbine tower, the aim of which is to accurately measure the response of the system in two directions. The natural frequency of the system is estimated from the analysis of the accelerometer record. The experimental work has two main parts, namely (a) the determination of the soil–structure interaction parameters k_l and k_r, and (b) the determination of the dynamic characteristics, namely the damping factor and the natural frequency. Once these values are known, the soil structure interaction parameters are used as 'input' to the analytical and numerical model so that the predicted natural frequencies can be compared to the experimental measurements.

Table 4
Properties of the Leighton Buzzard Fraction B sand.

Specific gravity of the soil solids (Gs)	2.65
Maximum void ratio (e_{max})	0.78
Minimum void ratio (e_{min})	0.486
Particle size (D_{50})	0.82 mm
Minimum dry unit weight	14.65 kN/m^3
Maximum dry unit weight	17.58 kN/m^3
Critical angle of friction ϕ_{cr}	34°

Table 5
Properties of the soils used in the test.

Soil type	Bulk density (kN/m^3)	Shear modulus (MPa)
Dry sand	15.73	12.72
Saturated sand	19.6	8.2
Clay (Kaolin powder mixed with water and consolidated)	16.6	2

3.2. Set-up and procedure for the testing

In this section we describe the test procedures used to derive the soil–structure interaction parameters necessary to apply the analytical approach discussed earlier. We also describe the procedure for the determination of the natural frequency which is necessary to validate the proposed simplified approach.

(1) *Static moment test to measure k_r*: The rotational stiffness of the foundation (k_r) was measured by applying a moment at the pile head and measuring the slope caused by it, see Fig. 6 for the set-up. The pile was carefully installed in the soil by pushing and was allowed sufficient time to reach the steady-state. The allowed time is particularly crucial for clayey soils as the pore pressure generated during the installation was allowed to dissipate. A known moment was applied at the top of the pile and the rotation of the pile head was obtained by measuring the lateral displacements of two 40 mm spaced dial gauges. Typical results for three different soil types are shown in Fig. 7. The initial tangent is considered as the stiffness as we are interested in the small-amplitude vibration.

(2) *Static displacement test to measure k_l*: The lateral stiffness of the foundation (k_l) was measured by carrying a lateral push over test on the embedded pile in the soil. Lateral load was applied at the top of the pile and the lateral displacements of

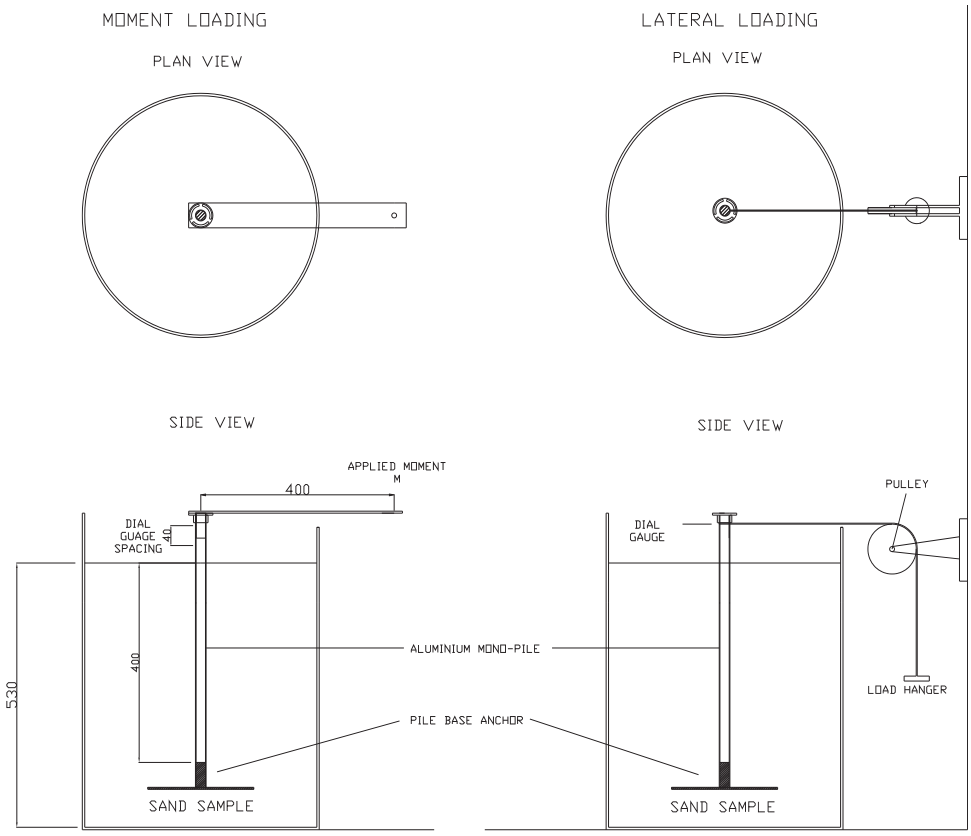

Fig. 6. Schematic diagram of the setup showing the measurements of k_l and k_r.

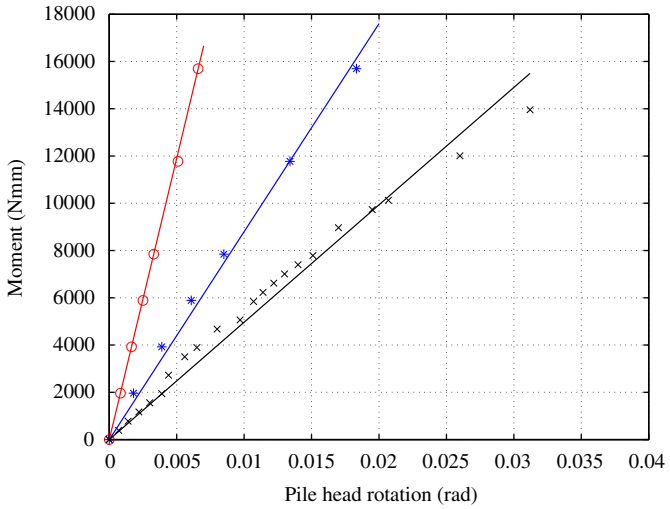

Fig. 7. Typical test results for k_r; '-o-' dry sand (linearised value 2.38 MNmm/rad); '-*-' saturated sand (linearised value 0.88 MNmm/rad); '-x-' clay (linearised value 0.49 MNmm/rad).

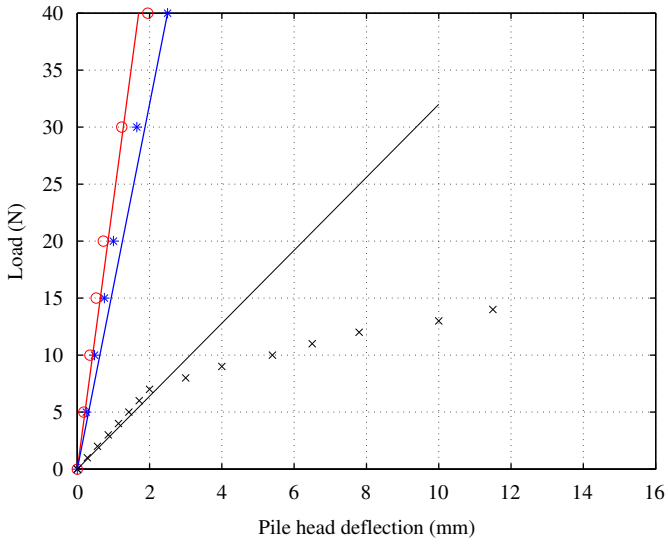

Fig. 8. Typical test results for k_l; '-o-' dry sand (linearised value 23.53 N/mm); '-*-' saturated sand (linearised value 16 N/mm); '-x-' clay (linearised value 3.2 N/mm).

the pile were measured using a dial gauge, see Fig. 6 for the set up. The load displacement curve is plotted and the initial tangent gives the value of k_l. Fig. 8 shows three typical test results for dry sand, saturated sand and clay.

(3) *Natural frequency and damping factor from the dynamic testing*: The natural frequency of the wind-turbine system was measured through the free vibration test. This was carried out by applying a small excitation to the system and consequently recording the acceleration. Fig. 9 shows a typical measured frequency response function in the lateral direction of the model wind turbine in sandy soil. The time-domain acceleration signals have been transformed using the Pwelch [21] method.

Seventeen tests were carried out under various conditions of loading as tabulated in Table 6. The pile was initially inserted into the soil and the static moment test and lateral tests were carried out to measure k_l and k_r. The wind turbine was then carefully fitted on the top of the pile to keep the soil disturbance to a minimum. The dynamic response of the system was measured by vibration testing. The actuator was fitted and the motor was connected to the power source. The blades were allowed to spin at 40 rpm so that 1P frequency is 0.67 Hz. The tests presented in Table 6 were carried out to study the long-term performance of the wind turbine model due to repeated cyclic loading. Test id 1 and 2 forms the same set of data, whereby test id 1 presents the initial condition and test id 2 presents the dynamic properties after 14,400 cycles. Similarly test id 5 through test id 8 form another sequence where the model turbine was cycled through 43,200 cycles of loading and measurements were taken after 14,400 cycles and then after 28,800 and finally after 43,200 cycles. The actuator attached to the tower was allowed to operate at 2 Hz, i.e. the 3P frequency. The amplitude of vibration was kept such that the displacement of the pile head is about 0.13–0.22 mm. This corresponds to 0.34–0.57% of the pile diameter which can be considered as small amplitude vibration. The tower was excited through the 1P and 3P frequencies for various number of cycles as tabulated in column 2 of Table 6. The motor and the actuator was stopped and natural frequency of vibration was measured. The wind turbine was again detached from the pile so that static moment test and push test could be carried out for the next set. In Table 6, the measured damping factors are also tabulated for all the 17 test cases. This has been obtained using the standard logarithmic decrement method [22]. More advanced methods for modeling and identification of damping using the modal damping factor are available, see for example [23,24].

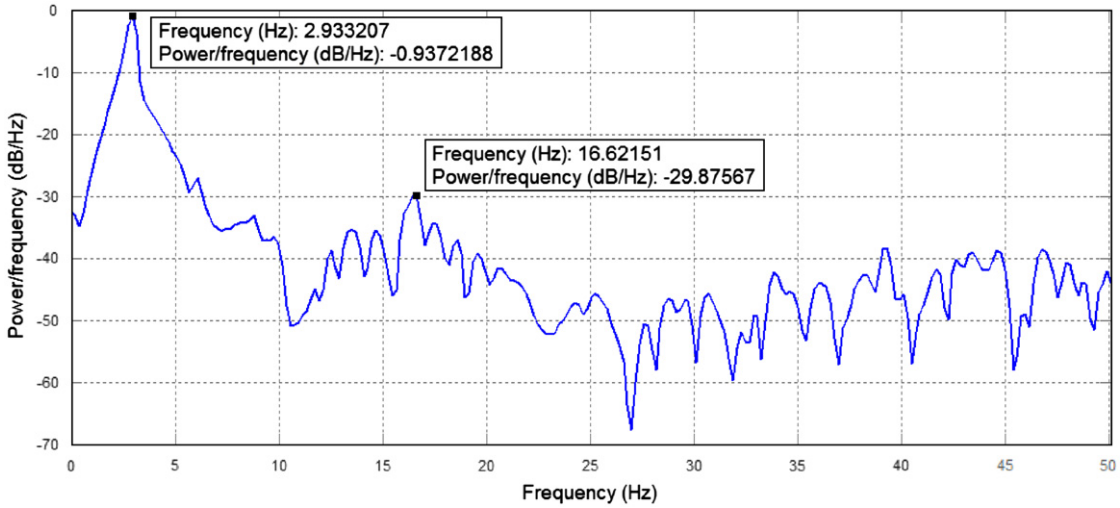

Fig. 9. A typical measured frequency response function in the lateral direction of the model wind turbine in sandy soil.

Table 6
Soil stiffness and damping parameters obtained from 17 tests conducted in this study.

Test id	Soil condition and the test condition	k_r (MN mm/rad)	k_l (N/mm)	η_r	η_l	Damping factor (%)
1	Dry sand: Pile embedded in the soil (initial condition)	2.38	28.3	1.12	13.32	3.18
2	Dry sand: Pile embedded in the soil and following 14,400 cycles of (3P) loading and 4800 cycles of (1P) loading	1.14	37.5	0.54	17.65	2.1
3	Saturated sand: Pile embedded in the soil (initial condition)	0.86	25	0.40	11.76	3.6
4	Saturated sand: Pile embedded in the soil and following 14,400 cycles of (3P) loading and 4800 cycles of (1P) loading	1.01	35.71	0.48	16.81	2.8
5	Dry sand (relative density): Pile embedded in the soil (initial condition)	0.7	22.06	0.33	10.38	2.68
6	Dry sand: Pile embedded in the soil and following 14,400 cycles of (3P) loading and 4800 cycles of (1P) loading	0.76	37.50	0.36	17.65	2.57
7	Dry sand: Pile embedded in the soil and following 28,800 cycles of (3P) loading and 9600 cycles of (1P) loading	0.799	41.67	0.37	19.61	2.8
8	Dry sand: Pile embedded in the soil and following 43,200 cycles of (3P) loading and 14,400 cycles of (1P) loading	0.904	50	0.43	23.53	2.5
9	Saturated sand (relative density): Pile embedded in the soil (initial condition)	0.88	20	0.42	9.41	3.8
10	Saturated sand: Pile embedded in the soil and following 14,400 cycles of (3P) loading and 4800 cycles of (1P) loading	0.98	27.4	0.46	12.89	3.07
11	Saturated sand: Pile embedded in the soil and following 28,800 cycles of (3P) loading and 9600 cycles of (1P) loading	1.01	31.25	0.48	14.71	2.96
12	Saturated sand: Pile embedded in the soil and following 43,200 cycles of (3P) loading and 14,400 cycles of (1P) loading	1.04	36.36	0.49	17.11	2.8
13	Dry sand (relative density): Pile embedded in the soil (initial condition)	1.06	20.20	0.50	9.51	3.23
14	Dry sand: Pile embedded in the soil and following 43,200 cycles of (3P) loading and 14,400 cycles of (1P) loading	1.35	26.67	0.64	12.55	2.94
15	Saturated sand (relative density): Pile embedded in the soil (initial condition)	0.81	16.81	0.38	7.91	2.88
16	Saturated sand: Pile embedded in the soil and following 43,200 cycles of (3P) loading and 14,400 cycles of (1P) loading	0.99	33.90	0.47	15.95	2.80
17	Clay: Pile embedded in soft clay (undrained strength 10 kPa)	0.428	3.5	0.201	1.65	19

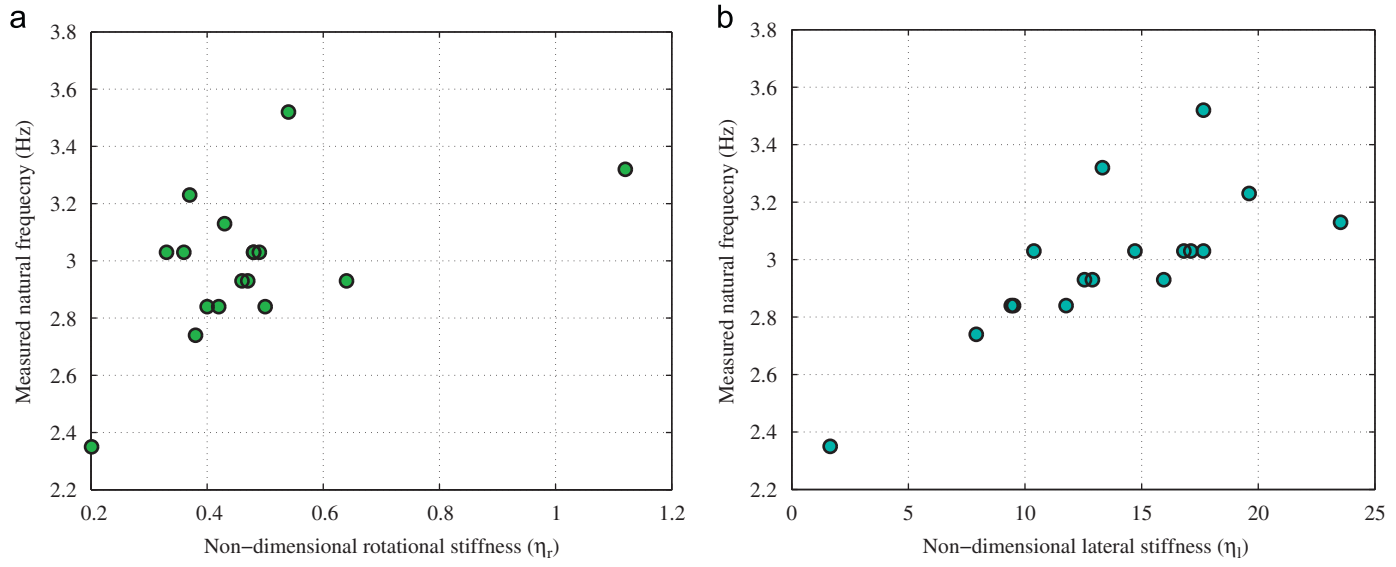

Fig. 10. The first natural frequency (Hz) obtained from the 17 test cases plotted separately against non-dimensional rotational and lateral stiffness of the foundation. The natural frequency of the system with fixed base is $f_{\text{fixedbase}} = 10.66$ Hz. (a) Variation with non-dimensional rotational stiffness (η_r). (b) Variation with non-dimensional lateral stiffness (η_l).

The effect of the soil properties on the natural frequencies is discussed in the next section.

4. Results and discussion

The test measurements are outlined in detail in Table 6. A wide variation in the values of k_l and k_r can also be seen in the results. Based on the theory developed in Section 3, a particular wind turbine will have a fixed value of α (the mass ratio of the turbine and the tower), ν (depending on the mass of the rotor-nacelle and stiffness of the tower) and the frequency scaling parameter c_0. For this scaled turbine: the value of $\alpha = 2.34$, $\nu = 0.007$ and $c_0/2\pi = 0.34$ Hz. The fixed base frequency of the wind turbine is measured as ($f_{\text{fixedbase}}$) 10.27 Hz. Tempel and Molenaar [3] gave the expression of the first natural frequency with fixed base as

$$f_1 \approx \sqrt{\frac{3.04EI}{(M + 0.227\ \text{mL})4\pi^2 L^3}}. \tag{14}$$

Calculation based on Eq. (14) gives a value of $f_{\text{fixedbase}} = 10.66$ Hz. The measured value is slightly lower than the theoretical prediction is perhaps due to the fact that full fixity could not be achieved in the experiments due to improper clamping of the base of the tower. Table 6 also provides the two soil–structure interaction (SSI) parameters, i.e. η_l and η_r for all the 17 tests. Fig. 10(a) shows the variation of the normalised first natural frequency with respect to η_r. On the other hand, Fig. 10(b) shows the normalised first natural frequency with respect to η_l. In Fig. 11 we show the variation of the measured damping factor plotted against non-dimensional rotational and lateral stiffness of the foundation. The damping factor for the foundation supported on clay (test id 17) is not shown here as the value is significantly higher (19%). One pattern that emerges from the experimental measurements in Figs. 10(b) and 11(b) is that the natural frequency increases with the increase in lateral stiffness and damping decreases with the increase in lateral stiffness. However, no such clear patterns emerges with respect to the variation in the rotational stiffness. The essential features observed through the analytical studies that could be captured in the experiments are as follows:

- The natural frequency of the wind turbine-foundation system is sensitive to the foundation flexibility. Therefore, it may not be appropriate to consider that the wind turbine is fixed at the base.
- Generally, there is an increase in the first natural frequency with the increase in the foundation stiffness.
- It may be observed that due to cyclic loading effects, the stiffness of the wind turbine system supported on sandy soil generally increased. For example, if we compare test id 9–12 the frequency of the system founded in saturated sand increased from 2.84 Hz to 3.03 Hz under the influence of 43,200 cycles of loading. This increase in stiffness of the system may be attributed due to the compaction of the granular material under the cyclic action. The overall damping of the system has been observed to decrease from 3.8% to 2.8%. This measure of damping is due to the components from the structure and the soil but the increase is more likely due to the soil–structure interaction.
- The damping of soft clay soil is greater than saturated sand (wet sand, i.e. typical offshore) which is again greater than dry sand. Typical value of observed overall damping for soft clay is 19% (based on one data). Average value of damping for saturated sand is 3.1% and 2.8% for dry sand.

In Table 7, we compare the first natural frequency (in Hz) obtained from the experiment, finite element methods and the proposed analytical method. For the finite element method, SAP 2008 has been used [25,26]. In the finite element model, 25 beam elements have been used with properties described in Table 2. Eigenvalue analysis in SAP is performed to obtain the natural frequency of the system. The values of the two soil–structure interaction (SSI) parameters, i.e. η_l and η_r, for all the 17 tests given in Table 6 are used in the analytical and finite element method. Percentage errors compared to the experiment results are shown in the table. Test case 1 (dry sand), showed maximum discrepancy from the experimental results. Fig. 12 compares the experimentally observed natural frequencies with the theoretical

Table 7
The first natural frequency (in Hz) obtained from the experiment, finite element methods and the proposed analytical method. The values in the parenthesis are percentage errors compared to the experiment results.

Test id	Experimental results	Finite element results	Analytical method
1	3.32	4.95 (49.0964)	4.78 (43.9097)
2	3.52	3.76 (6.8182)	3.62 (2.8740)
3	2.84	3.32 (16.9014)	3.18 (12.0461)
4	3.03	3.57 (17.8218)	3.43 (13.2477)
5	3.03	3.03 (0)	2.90 (−4.1883)
6	3.03	3.16 (4.2904)	3.04 (0.1763)
7	3.23	3.24 (0.3096)	3.10 (−4.0006)
8	3.13	3.42 (9.2652)	3.28 (4.8143)
9	2.84	3.34 (17.6056)	3.20 (12.8415)
10	2.93	3.52 (20.1365)	3.38 (15.2289)
11	3.03	3.57 (17.8218)	3.43 (13.0437)
12	3.03	3.62 (19.4719)	3.48 (14.7311)
13	2.84	3.61 (27.1127)	3.47 (22.2550)
14	2.93	4.01 (36.8601)	3.86 (31.6121)
15	2.74	3.22 (17.5182)	3.08 (12.5032)
16	2.93	3.54 (20.8191)	3.40 (16.1349)
17	2.35	2.32 (−1.1925)	2.76 (17.6359)

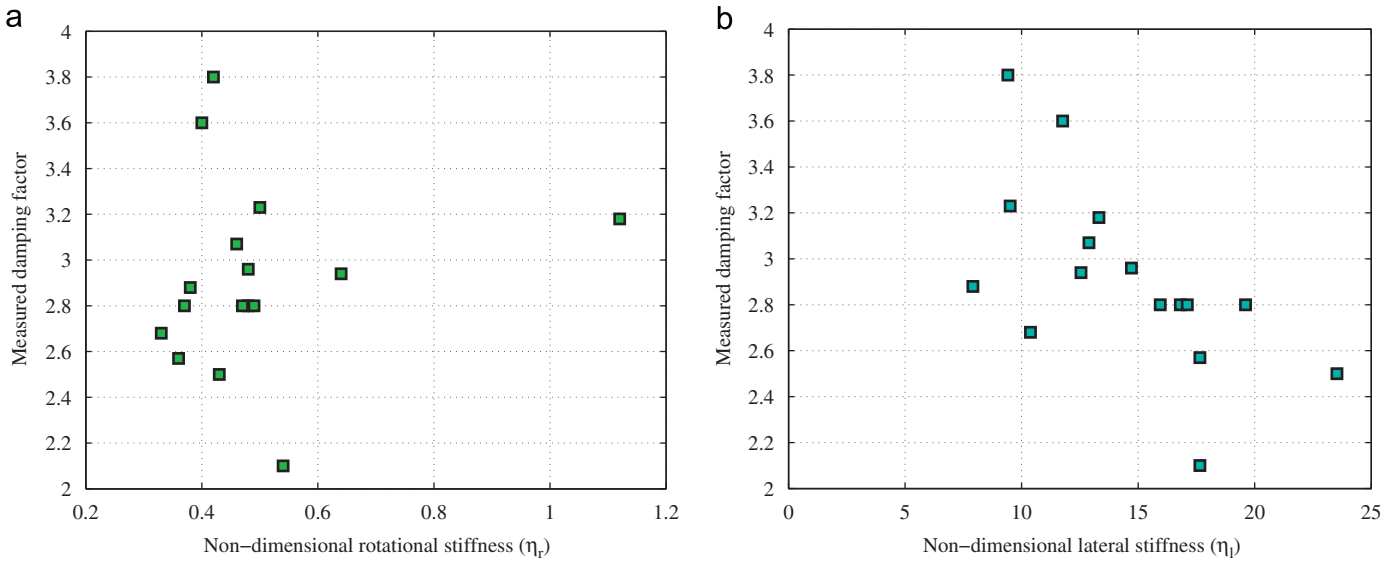

Fig. 11. The damping factor obtained from the 17 test cases plotted separately against non-dimensional rotational and lateral stiffness of the foundation. The damping factor for the foundation supported on clay (test id 17) is not shown here as the value is significantly higher (19%). (a) Variation with non-dimensional rotational stiffness (η_r). (b) Variation with non-dimensional lateral stiffness (η_l).

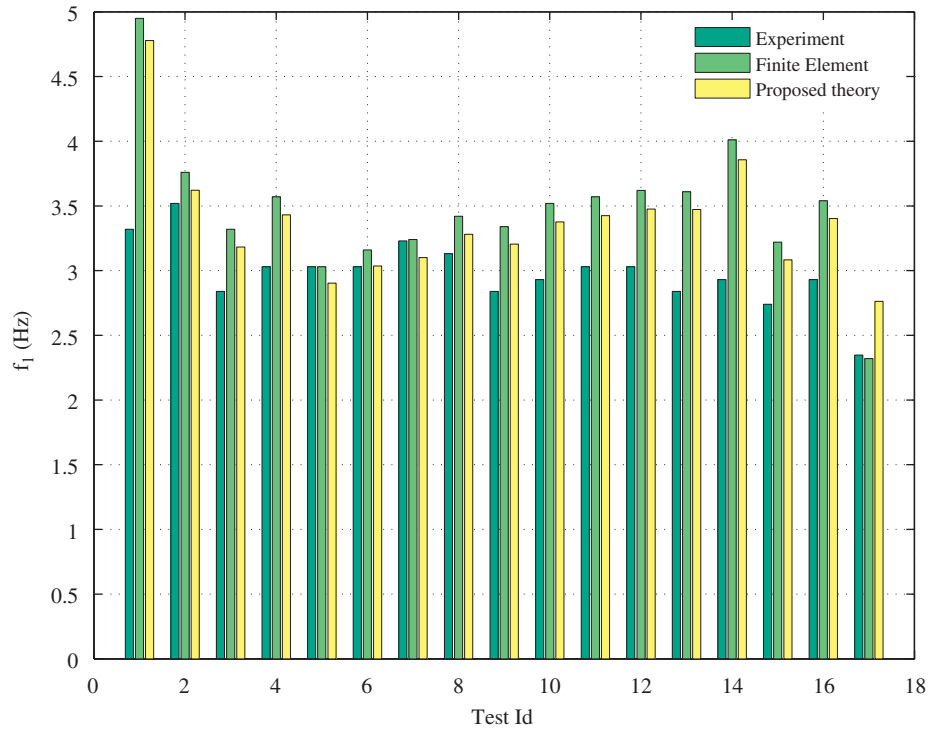

Fig. 12. Comparison between experimentally observed natural frequencies and theoretical predictions for 17 test cases. See Table 6 for the details of the 17 test cases.

predictions. The finite element prediction and the proposed theoretical results are close for all the 17 test cases.

The theoretical and numerical natural frequencies generally showed higher values compared to the experimental natural frequencies. The possible reasons for such discrepancies may be as follows:

- In the theoretical analysis, the stiffness of the soil is taken into consideration but the mass of the soil is ignored. While this assumption is widely accepted for static analysis, some doubts may be raised for similar assumptions in dynamic analysis. If the mass of the soil is considered in the analysis, the frequency of the system would decrease which may explain the reason for this apparent overestimation. However, there are no published recommendations in this regard.
- The theoretical analysis predicts the undamped frequency of vibration of the system, i.e. the damping of the system is not taken into consideration. However, the real system has some damping and the observed frequency is damped frequency. Undamped frequency being lower than the damped frequency may explain part of the reason for overestimation of the theoretical results.

From Fig. 12 we conclude that the simple analytical approach taken here predicts the general trend of the experimental results with reasonably good accuracy. Moreover, the analytical results also agree well with detailed finite element results.

5. Conclusions

This paper presents an analytical and experimental study on the dynamics of a model wind turbine considering the flexibility of foundation. The free-vibration analysis, which is a necessary first-step for dynamic analysis, is considered. The study shows that the frequency of vibration is strongly related to the stiffness of the foundation. A simplified analytical method is suggested to estimate the natural frequencies of the system. The proposed analytical method is validated using the 1:100 scale model turbine and the finite element method. New test methods have been developed to obtain two soil–structure interaction parameters, namely, the normalised rotational and lateral stiffness parameters. These quantities are used as inputs to the analytical approach. Natural frequencies and damping factors of the model system have been obtained for 17 different cases using dynamic testing. Analytical results for the natural frequencies provide a fair match to the experimental results. Generally it has been observed that analytical and finite element results overestimate the natural frequency. Some possible reasons for such discrepancies have been outlined. The experimental and analytical investigations carried out here show the need for further research on modeling the soil for the dynamic analysis of large offshore wind turbines. The study taken here considers limited (17 in this case) test cases. However, the novel testing procedure and the analytical developments are general in nature and can be applied to a wide range of wind turbine structures. Future research is needed to explore the validity of the methods developed in this paper to practical cases.

Acknowledgments

The model test setup and the tests has been carried out by Peter Baldwin, Andrew Crockett and Juan Monino Ramirez (Erasmus student from Spain) at the University of Bristol as a part of their academic project. The financial support provided by I.Struct.E is acknowledged. S.A. gratefully acknowledges the support of The Royal Society of London through the Wolfson Research Merit award.

References

[1] Carter J. North hoyle offshore wind farm: design and build. Energy: Proceedings of the Institution of Civil Engineers EN1 2007; 21–29.

[2] DnV, Guidelines for design of wind turbines-DnV/Riso, Code of practice, DnV, USA, 2001.
[3] Tempel D-P, Molenaar D-P. Wind turbine structural dynamics—a review of the principles for modern power generation, onshore and offshore. Wind Engineering 2002;26(4):211–20.
[4] Bhattacharya S, Madabhushi SPG, Bolton MD. An alternative mechanism of pile failure in liquefiable deposits during earthquakes. Géotechnique 2004;54(3):203–13.
[5] Vucetic M, Dobry R. Effect of soil plasticity on cyclic response. Journal of Geotechnical Engineering 1991;117(1):3–10.
[6] Adhikari S, Bhattacharya S. Dynamic analysis of wind turbine towers on flexible foundations. Shock and Vibration, in press, doi:10.3233/SAV-2010-0615.
[7] Adhikari S, Bhattacharya S. Vibrations of wind-turbines considering soil–structure interaction. Wind and Structures, An International Journal, in press.
[8] Géradin M, Rixen D. Mechanical vibrations. 2nd ed. New York, NY: John Wiley & Sons; 1997. [translation of: Théorie des Vibrations].
[9] Kreyszig E. Advanced engineering mathematics. 9th ed. New York: John Wiley & Sons; 2006.
[10] Adhikari S, Bhattacharya S. Dynamic instability of pile-supported structures in liquefiable soils during earthquakes. Shock and Vibration 2008;15(6):665–85.
[11] Bhattacharya S, Adhikari S, Alexander NA. A simplified method for unified buckling and dynamic analysis of pile-supported structures in seismically liquefiable soils. Soil Dynamics and Earthquake Engineering 2009;29(8):1220–35.
[12] Huang TC. The effect of rotatory inertia and of shear deformation on the frequency and normal mode equations of uniform beams with simple end conditions. Transactions of ASME, Journal of Applied Mechanics 1961;28:579–84.
[13] Chen Y. On the vibration of beams or rods carrying a concentrated mass. Transactions of ASME, Journal of Applied Mechanics 1963;30:310–1.
[14] Gurgoze M, Erol H. On the frequency response function of a damped cantilever simply supported in-span and carrying a tip mass. Journal of Sound and Vibration 2002;255(3):489–500.
[15] Oz HR. Natural frequencies of an immersed beam carrying a tip mass with rotatory inertia. Journal of Sound and Vibration 2003;266(5):1099–108.
[16] Elishakoff I. Eigenvalues of inhomogeneous structures: unusual closed-form solutions. Boca Raton, FL, USA: CRC Press; 2005.
[17] Elishakoff I. Essay on the contributors to the elastic stability theory. Meccanica 2005;40(1):75–110.
[18] Gurgoze M. On the eigenfrequencies of a cantilever beam carrying a tip spring-mass system with mass of the helical spring considered. Journal of Sound and Vibration 2005;282(3–5):1221–30.
[19] Wu JS, Hsu SH. A unified approach for the free vibration analysis of an elastically supported immersed uniform beam carrying an eccentric tip mass with rotary inertia. Journal of Sound and Vibration 2006;291(3–5):1122–47.
[20] Bhattacharya S, Lombardi D, Muir Wood D. Similitude relationships for physical modelling of monopile-supported wind turbines. International Journal of Physical Modelling in Geotechnics 2011;11(1).
[21] Welch PD. The use of fast fourier transform for the estimation of power spectra—a method based on time averaging over short modified periodgram. IEEE Transactions on Electro acoustics 1967;15:7–73.
[22] Meirovitch L. Principles and techniques of vibrations. New Jersey: Prentice-Hall International, Inc.; 1997.
[23] Papagiannopoulos GA, Beskos DE. On a modal damping identification model of building structures. Archive of Applied Mechanics 2006;76(7–8):443–63.
[24] Adhikari S. Damping modelling using generalized proportional damping. Journal of Sound and Vibration 2006;293(1–2):156–70.
[25] Dash SR, Govindaraju L, Bhattacharya S. A case study of damages of the Kandla Port and Customs Office tower supported on a mat-pile foundation in liquefied soils under the 2001 Bhuj earthquake. Soil Dynamics and Earthquake Engineering 2009;29(2):333–46.
[26] Dash SR, Bhattacharya S, Blakeborough A. Bending-buckling interaction as a failure mechanism of piles in liquefiable soils. Soil Dynamics and Earthquake Engineering 2010;30(1–2):32–9.